Features of steel protection by chamber inhibitors based on a mixture of octadecylamine and benzotriazole

A.V. Karaulova, A.Yu. Luchkin, O.A. Goncharova and N.N. Andreev*

A.N. Frumkin Institute of Physical Chemistry and Electrochemistry, Russian Academy of Sciences, Leninsky pr. 31, 119071 Moscow, Russian Federation
**E-mail: n.andreev@mail.ru*

Abstract

The study investigated the impact of the octadecylamine to benzotriazole ratio on the effectiveness of their mixture as a chamber inhibitor for steel corrosion, using both corrosion and electrochemical methods. It is established that the anticorrosive after-effect of the mixture depends on the ratio of its components. The inhibitor that contains 75% octadecylamine exhibits the best protective properties. The use of a mixture of octadecylamine and benzotriazole in the chamber treatment of steel is characterized by antagonism of the protective action, but the inhibitor of optimal composition is significantly more effective than the individual components. The antagonism of the protective effect of octadecylamine and benzotriazole may be related to acid-base interactions of these compounds, which results in a decrease in the inhibitor's vapor pressure. The protective effect of the mixture of octadecylamine and benzotriazole is due to the stabilization of the passive state of the steel, manifested by an increase in the pitting potential and/or anti-pitting basis in chloride-containing electrolytes. The mechanism of action of the studied mixture is "blocking-activation" with a predominance of blocking effects.

Received: March 20, 2024. Published: March 29, 2024 doi: 10.17675/2305-6894-2024-13-2-2

Keywords: *carbon steel, atmospheric corrosion, chamber corrosion inhibitor, mixed corrosion inhibitor.*

1. Introduction

Protection of metals from atmospheric corrosion is an important technical challenge [1–8]. One method of addressing this issue is through the use of inhibitors [8–13]. Among them, vapor-phase inhibitors – volatile (VCI) and chamber inhibitors (CIN) – are distinguished by their efficiency and manufacturability.

Numerous publications [14–25] focus on the theory and practice of metal protection using VCI. CINs have been studied less. The method of chamber treatment (CT) of metals was developed at the Institute of Physical Chemistry and Electrochemistry of the Russian Academy of Sciences only a few years ago. However, the advantages of CIN over VCI are already apparent, and its potential for use in industry is promising.

CT involves exposing of metal products to vapors of low-volatile inhibitors under normal conditions in a sealed chamber at elevated temperatures (t) [26–30]. During CT, nano-sized adsorption layers of inhibitors are formed on the metal from the vapor phase,

which can prevent atmospheric corrosion for a long time after removing the products from the chamber.

An effective chamber inhibitor for atmospheric corrosion of steel is a mixture of octadecylamine (ODA) and 1,2,3-benzotriazole (BTA). Both components are low toxic and characterized by low vapor pressure at room temperature. However, when the chamber is heated to 120°C, the vapor pressure of these compounds increases by several orders of magnitude and their mixture acquires the volatility necessary for vapor phase protection. The anticorrosion properties of this CIN were investigated in [27]. Nevertheless, the authors did not analyze the influence of the ratio of the mixture components on the protection efficiency, assuming that ODA and BTA do not interact with each other. Indeed, in the absence of component interactions, the vapor composition of blended CINs, which determines the protection efficiency, does not depend on their ratio. Nevertheless, the interaction of ODA and BTA in the inhibitor volume, in the gas phase and adsorption layers cannot be excluded *a priori*.

The aim of this work was to investigate the effect of the ratio of ODA and BTA on the protective effect of a mixed chamber inhibitor against steel.

2. Experimental

All the reagents used in this study were of “pure” or “chemical pure” grade. Portions of the blended CINs were prepared by grinding its components.

In this work, samples and cylindrical electrodes made of low-carbon steel St3 were used. All the samples measured 30×50×3 mm and had a hole for mounting in chambers and in test cells.

The cylindrical electrodes were 10 mm in diameter. One end of the cylinders had a threaded hole for a rod holder. The electrodes were pressed into a Teflon cage to prevent interaction of the side surface with the electrolyte. The lower ends served as the working surface.

Sample and electrode preparation

The working surfaces of the samples and electrodes were ground with sandpaper of grit from P240 to P1500, degreased with acetone and dried in air. Then they were mounted on nylon threads to the lids of 0.7 litre glass cells containing a portion (1 g) of CIN. The cells were hermetically sealed and placed in a SNOL 50/350 drying oven heated to 120°C. The duration of CT was 1 hour. Afterwards, the cells were cooled, opened, and left at room temperature for 24 hours. The specimens and electrodes were then removed and tested.

Accelerated corrosion tests under conditions of daily moisture condensation

Samples were attached to nylon threads from the lids of 0.7 litre glass test cells, ensuring that they did not touch the walls of the cell or each other. Each cell was filled with 50 ml of hot (50°C) water, which caused intensive condensation of moisture on the metal. The cooled

water was replaced with hot water once a day. The samples were inspected hourly for two days from the start of the test. Then the surface condition was monitored every 6 hours. The recorded time of the first appearance of corrosion damage on the metal surface (τ_{prot}) was noted.

The mutual influence of the components of the mixtures in corrosion tests was evaluated by the coefficient α:

$$\alpha = \tau_{prot,ex}^{ODA+BTA} / \tau_{prot,calc}^{ODA+BTA},$$

where the index "ex" refers to the value of τ_{prot} of the mixture of ODA and BTA determined experimentally, while "calc" refers to the result of calculation according to the formula:

$$\tau_{prot,calc}^{ODA+BTA} = \tau_{prot}^{ODA} \cdot \tau_{prot}^{BTA} / \tau_{prot}^{IS}$$

which was derived under the assumption that there is no interaction between the components of the mixture. Here τ_{prot}^{IS} is time to the appearance of corrosion on the samples in the initial state (IS).

According to [28], the value $\alpha = 1$ indicates the absence of interaction between the mixture components, $\alpha > 1$ indicates synergism, while $\alpha < 1$ indicates antagonism of the protective effect.

Potentiodynamic polarization study

Anodic polarization curves were obtained using an IPC-Pro MF potentiostat (Russia). Experiments were carried out in a three-electrode cell. A graphite electrode was used as a counter electrode. Potentials (E) were measured relative to the saturated silver chloride electrode and converted to the normal hydrogen scale. Borate buffer solution with pH=7.36 containing 0.001 M NaCl served as the electrolyte. The experiments were carried out at room temperature and natural aeration of the solution.

The electrodes were placed in a cell with electrolyte and kept for 5 min until E stabilized (E_0). After that, they were polarized anodically at a sweep rate of 0.2 mV/s. The pitting potential (E_{pit}) was taken as E at which the anodic current density (i) reached 0.002 mA/cm^2.

Electrochemical impedance spectroscopy

The impedance experiments were performed using a potentiostat, cell and electrolyte similar to those described above, and a FRA-2 module. Impedance was measured in the potentiostatic mode at E_0 with imposition of a harmonic signal in the frequency range of $0.1–10^5$ Hz at an amplitude of 10 mV.

The electrochemical impedance spectra were interpreted in terms of the modified Mansfeld equivalent circuit [31, 32] shown in Figure 1.

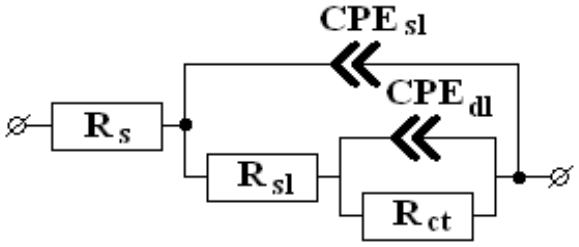

Figure 1. Equivalent circuit.

In this circuit: R_s is the resistance of the bulk electrolyte between the counter electrode and working electrode, which does not affect the electrode processes and depends on the conductivity of the medium and the geometry of the cell; R_{sl} is the resistance of the surface oxide-hydroxide and adsorption layers; R_{ct} is the polarization resistance, which characterizes the electrochemical kinetics of the corrosion process; CPE_{sl} is the constant phase element, which characterizes the capacitance of the surface oxide and/or adsorption layers; and CPE_{dl} is the constant phase element, which reflects the capacitance of the electrical double layer. The impedance of the constant phase element was described by equation [34]:

$$Z_{CPE} = A^{-1}(j\omega)^{-n},$$

where: A is the proportionality factor; j is the imaginary unit; ω is the complex frequency related to the alternating current frequency; and n is an exponent representing the phase deviation, $0 \leq |n| \leq 1$.

The equivalent circuit parameters were calculated using Dummy Circuits Solver Version 2.1 [34].

The degree of protection of steel electrodes upon CT was determined by the formula:

$$Z = (R^{CT,TT} - R^{IS})/R^{CT,TT} \times 100\%$$

where $R^{CT,TT}$ is the sum of active resistances R_{ct} and R_{sl} in the equivalent circuit for the metal sample after CT or thermal treatment (TT). Similarly, R^{IS} is the sum of R_{ct} and R_{sl} for experiments with steel in the IS.

The experimental data matched the calculated ones to within at least 98%.

3. Results

Accelerated corrosion tests under conditions of daily moisture condensation

The results of corrosion tests carried out under conditions of daily moisture condensation are shown in Table 1.

On the samples of steel grade St3 in the IS and those subjected to TT without CIN, the first corrosion damages (rust plaque) were observed after 0.5 hours.

CT in BTA vapors slightly inhibited corrosion initiation. CT with ODA extended the time of full metal protection up to 120 hours.

Table 1. The τ_{prot} of adsorption films formed on steel at different treatment variants, and coefficients of mutual effect of components of blended CINs.

Treatment conditions	τ_{prot}, h	α
IS	0.5	–
TT without CIN	0.5	–
BTA 100%	3	–
ODA 100%	120	–
ODA 25% + BTA 75%	51	0.07
ODA 50% + BTA 50%	110	0.15
ODA 75% + BTA 25%	144	0.2

The protective aftereffect (PA) of the mixed CIN depended on the ratio of inhibitor components. With the increase in the content of ODA from 0 to 75%, the values of τ_{prot} increased from 3 to 144 hours. Note that the mixture containing 75 percent of ODA had the best protective properties and was superior to the components in terms of anti-corrosion properties. According to [28], this can occur even in the presence of component antagonism. Indeed, the calculated values of the α were significantly less than 1, indicating the antagonism of ODA and BTA in the chamber protection of steel. It is logical to assume that such antagonism is a consequence of the interaction of weak bases (ODA) and acid (BTA) in the CIN mixture. Such acid-base interactions are accompanied by a decrease in the vapor pressure of the inhibitor component and, consequently, in the efficiency of chamber protection.

Potentiodynamic polarization study

The data about the PA of the CIN obtained during corrosion experiments are in agreement with the results of potentiodynamic studies.

Figure 2 shows anodic polarization curves of steel electrodes at different variants of their treatment. In all cases, the curves had the appearance characteristic of the passive metal.

The E_0 of the electrodes in the IS was 0.035 V (Table 2). The passive film breakdown occurred at $E_{pit} = 0.250$ V (Table 2). The total extent of the passive region (anti-pitting basis, $\Delta E = E_{pit} - E_0$) was 0.215 V.

TT without CIN slightly ennobled both characteristic E values but almost did not affect the ΔE value.

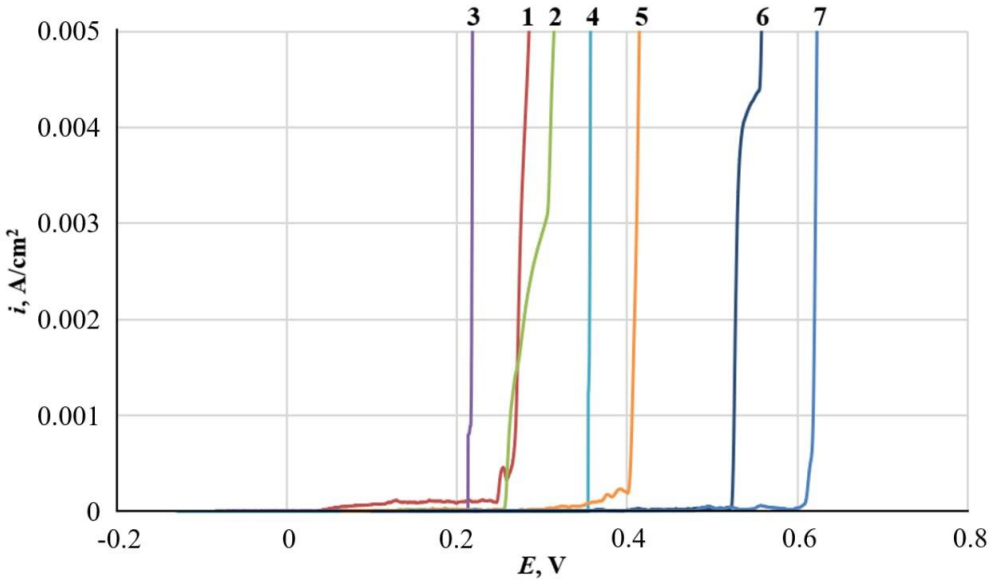

Figure 2. Anodic polarization curves of steel at different variants of its treatment: 1 – IS, 2 – TT without CIN, 3 – BTA, 4 – ODA, 5 – ODA 25% + BTA 75%, 6 – ODA 50% + BTA 50%, 7 – ODA 75% + BTA 25%.

Table 2. The effect of steel treatment in CIN vapor on the characteristics of anodic polarization curves.

Treatment conditions	E_0, V	E_{pit}, V	ΔE, V
IS	0.035	0.250	0.215
TT without CIN	0.070	0.280	0.210
BTA 100%	–0.085	0.210	0.295
ODA 100%	–0.130	0.345	0.475
ODA 25% + BTA 75%	0.065	0.400	0.335
ODA 50% + BTA 50%	0.145	0.520	0.375
ODA 75% + BTA 25%	0.020	0.610	0.590

CT of steel in BTA vapor shifted the E_0 values to the cathodic side. At the same time, the passive film breakdown was facilitated. The E_{pit} values in this treatment were lower than E_{pit} values for steel in IS and steel subjected to TT without CIN. However, the values of ΔE slightly increased.

After treatment of steel with ODA vapors, the E_0 was more enriched than when the electrodes were treated with BTA. The breakdown of the passive film was noticeably hampered. The values of E_{pit} and ΔE were 0.345 and 0.475 V, respectively.

The PA of the adsorption films of the mixed inhibitor increased symbatically with the content of ODA in it. As in the series of corrosion experiments, the best protection of steel ($E_{pit} = 0.61$ V and $\Delta E = 0.59$ V) was characterized by the CIN consisting of 75% of ODA. It

should be noted that the protective properties of this inhibitor exceeded the protective properties of ODA itself.

Thus, irrespective of the choice of potential E_{pit} or potential ΔE as a protection criterion, the data of potentiodynamic studies confirm the conclusions of corrosion experiments. The PA of blended CINs depended on the ratio of components. The best anti-corrosion properties were possessed by the inhibitor containing 75% of ODA.

Electrochemical impedance spectroscopy

Electrochemical impedance spectroscopy provides additional information on the protective effect of the CIN.

The Nyquist diagrams of steel electrodes at different variants of treatment are shown in Figure 3. Two semicircles appear on all hodographs with different degrees of distinctness. This allows us to apply for their description the Mansfeld scheme characterized by two time constants. Its parameters for different experiments are given in Table 3.

Table 3. Parameters of the equivalent circuit at different variants of steel electrode processing.

Treatment conditions	R_s, kΩ·cm^2	CPE_{sl}, S·s^n/cm^2	n_{sl}	R_{sl}, kΩ·cm^2	CPE_{dl}, S·s^n/cm^2	n_{dl}	R_{ct}, kΩ·cm^2	Z, %
IS	0.95	$3.41\cdot10^{-5}$	1.00	7.80	$4.39\cdot10^{-5}$	0.89	58.0	–
TT without CIN	0.46	$6.87\cdot10^{-6}$	0.88	76.4	$2.62\cdot10^{-5}$	1.00	76.0	56.9
BTA 100%	0.47	$9.02\cdot10^{-7}$	0.91	106	$6.87\cdot10^{-6}$	0.67	402	87.0
ODA 100%	0.59	$9.71\cdot10^{-7}$	0.85	209	$4.27\cdot10^{-6}$	1.00	441	89.9
ODA 25% + BTA 75%	0.57	$2.91\cdot10^{-6}$	0.91	179	$2.81\cdot10^{-6}$	0.92	588	91.4
ODA 50% + BTA 50%	0.59	$1.23\cdot10^{-6}$	0.92	207	$2.05\cdot10^{-6}$	0.98	926	94.2
ODA 75% + BTA 25%	0.96	$6.77\cdot10^{-7}$	0.93	555	$9.79\cdot10^{-7}$	0.64	2880	98.1

For steel electrodes in the IS, the value of R_{sl} is significantly less than R_{ct}. This suggests that the corrosion resistance of the metal is determined by the rate of electrode reactions in the double layer. The capacitive loop in the high-frequency region is due to the presence of air-formed oxide film on the surface. The values of n_{sl} and n_{dl} show that the constant phase elements represent pure capacitance.

TT of the electrode led to a decrease in the CPE_{sl} value compared to the IS of steel due to the growth of oxide on the surface. At the same time, the R_{sl} values increased almost 10 times. Comparison of CPE_{dl} values of the steel electrode before and after TT indicates a 2 times decrease in the electrochemically active surface of the metal. TT was accompanied by an increase in R_{ct} by 1.3 times. The growth of corrosion resistance of steel after TT was a consequence of thickening of oxide film. The values of n_{sl} and n_{dl} did not actually change after TT, which indicates the homogeneity of the oxide film and the absence of diffusion limitations in the course of electrode processes in the double layer. The Z of steel due to TT was 56.9%.

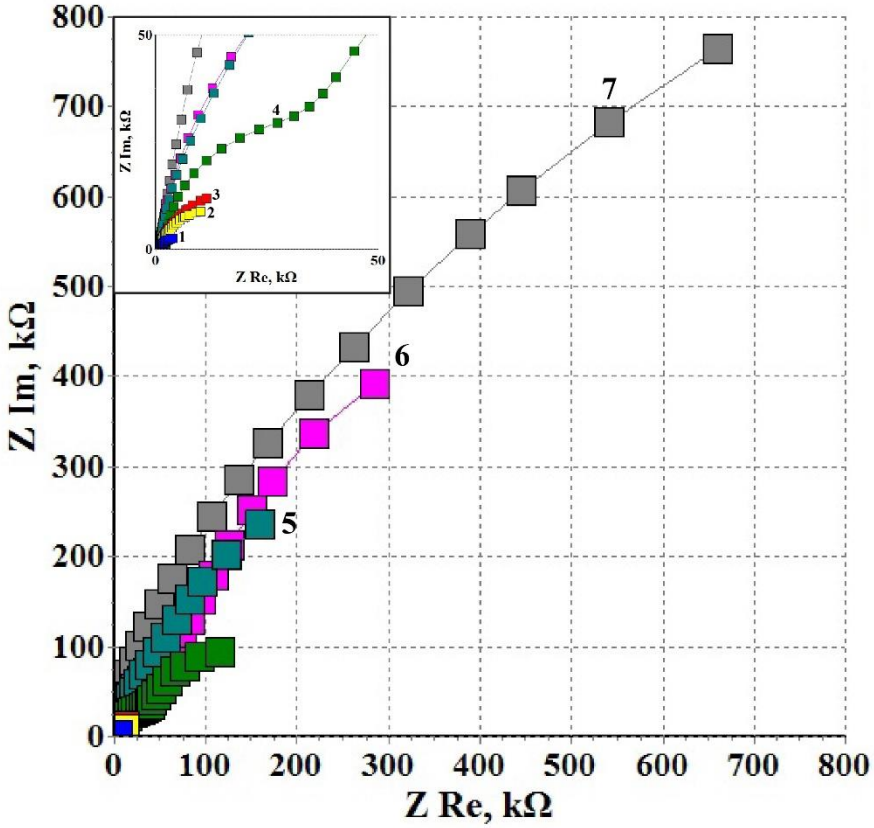

Figure 3. Nyquist diagrams of steel electrodes at different variants of its treatment: 1 – IS, 2 – TT without CIN, 3 – BTA, 4 – ODA, 5 – ODA 25% + BTA 75%, 6 – ODA 50% + BTA 50%, 7 – ODA 75% + BTA 25%.

CT of the steel electrode in BTA vapors led to a 2 orders of magnitude decrease in CPE_{sl}, due to the formation of adsorption films. They exhibited higher resistivity compared to the surface layers on the steel in the IS and after TT. The CPE_{dl} values also decreased by an order of magnitude. This was accompanied by an increase in polarization resistance by a factor of approximately 9. The value of n_{sl} was close to 1 due to the homogeneity of the surface films. At the same time, the value of n_{dl} shows that the electrode processes are inhomogeneous or complicated by diffusion. The degree of protection by BTA steel did not exceed 87%.

CT of steel with ODA also led to a decrease in CPE_{sl} and CPE_{dl} values. Moreover, the values of n_{sl} and n_{dl} indicate the homogeneity of surface layers and electrode processes in the double layer. The value of R_{sl} after treatment in ODA vapors was about 2 times higher compared to BTA, and the values of R_{ct} were commensurate for both inhibitors. It can be concluded that ODA slows down the rate of electrode reactions. At the same time, the blocking effect of the ODA film is greater than in the case of BTA. The value of Z for ODA was 89.9%.

CT in vapor mixtures was accompanied by a greater decrease in CPE_{sl} and CPE_{dl}, as well as an increase in R_{sl} and R_{ct}, compared to the components. The values of n_{sl} and n_{dl} show that the surface films are homogeneous and the electrode processes are not complicated by diffusion in all cases except for the mixture containing 75% of ODA. In this case, the n_{dl} value indicates diffusion limitations or inhomogeneity of processes in the double layer. In terms of steel protection efficiency, the blended CINs were superior to the components. For all mixtures studied, Z were above 90%. The most effective steel protection ($Z = 98.1\%$) was provided by the mixture containing 75% of ODA.

Thus, the data of electrochemical impedance spectroscopy agree with the results of corrosion and voltammetric experiments. PA of blended CINs depended on the ratio of components. The best anti-corrosion properties were possessed by the inhibitor containing 75% of ODA.

In addition, EIS allows us to make some conclusions about the mechanisms of CIN action.

Two mechanisms of corrosion inhibition are known: blocking and activation [11]. Inhibitors acting according to the first mechanism reduce the corrosion rate by decreasing the area of the active surface of the metal. At the same time, the corrosion rate on unblocked areas of the surface does not change. Activation mechanism means inhibition of corrosion by changing the kinetics of corrosion processes, *i.e.* accompanied by a change in their activation energy. Usually both mechanisms are realized simultaneously, but their contribution to the inhibitor action may be different.

In accordance with [28], the contribution of the blocking mechanism of inhibitor action to metal protection when using the equivalent scheme shown in Figure 1 is characterized by the value of R_{sl}. In this case, the corrosion inhibition coefficient due to blocking by surface layers (γ_{bl}) is the ratio of the resistance R_{sl} of the electrode after its TT or CT to the value of R_{sl}, for the metal in the IS:

$$\gamma_{block} = R_{sl}^{TT,CT} / R_{sl}^{IS}$$

The inhibition coefficient of electrochemical reaction using CIN (γ_{act}) is defined as the ratio of polarization resistances R_{ct} for samples after TT or CT and steel in IS:

$$\gamma_{act} = R_{ct}^{TT,CT} / R_{ct}^{IS}$$

The values of γ_{block} and γ_{act} for different variants of steel treatment are given in Table 4. Their comparison allows us to conclude about the mixed “blocking-activation” mechanism of action of the studied CINs. However, under all conditions of steel treatment the inequality $\gamma_{act} < \gamma_{block}$ is observed, which indicates the predominance of the blocking mechanism.

Table 4. Coefficients of steel corrosion inhibition by blocking and activation mechanism at different treatment variants.

Treatment conditions	γ_{block}	γ_{act}
TT without CIN	9.80	1.31
BTA 100%	13.6	6.93
ODA 100%	26.8	7.60
ODA 25% + BTA 75%	22.9	10.1
ODA 50% + BTA 50%	26.5	16.0
ODA 75% + BTA 25%	71.1	49.7

Conclusions

1. The protective aftereffect of the mixture of ODA and BTA depends on the ratio of components. The best corrosion protection is provided by CIN with 75% ODA.
2. The mixture of ODA and BTA in chamber protection of steel is characterized by antagonism of protective action, but the CIN with optimal composition is markedly superior to the components in terms of effectiveness.
3. The antagonism of the protective effect of ODA and BTA may be related to acid-base interactions of these compounds accompanied by a decrease in the vapor pressure of CIN.
4. The protective effect of the mixture of ODA and BTA is due to the stabilization of the passive state of steel, demonstrated by an increase in the pitting potential or anti-pitting base in chloride-containing electrolytes.
5. The mechanism of action of the ODA/BTA mixture is “blocking-activation” with predominance of blocking effects.

Funding

This study was financially supported by the Russian Science Foundation (Grant No. 23-23-00092 “Development of scientific principles of self-organization of protective nanoscale films of organic inhibitors on the surface of metals and alloys from the vapor-gas phase”).

References

1. A.A. Mikhailov, Yu.A. Panchenko and Yu.I. Kuznetsov, *Atmospheric Corrosion and Metal Protection*, Tambov, Izd-vo R.V. Pershin, 2016, 555 pp. (in Russian).
2. I.L. Rosenfeld, *Atmospheric Corrosion of Metals*, Moscow, Izd-vo AS USSR, 1960, 372 pp. (in Russian).
3. Yu.N. Mikhailovsky, *Atmospheric corrosion of metals and methods of their protection*, Moscow, Metallurgiya, 1989, 102 pp. (in Russian).
4. W.D. Wui, *Atmospheric corrosion of metals in the tropics*, Moscow, Nauka, 1994, 240 pp. (in Russian).

5. S.K. Chawla and J.H. Payer, *Atmospheric corrosion: A comparison of indoor vs. outdoor*, Proceedings 11th Int. Corros. Congr, 1990, pp. 2–17.
6. C. Leygraf, I.O. Wallinder, J. Tidblad and T. Graedel, *Atmospheric Corrosion*, 2nd ed., New Haven, CT, USA, 2016, p. 152.
7. C. Leygraf and T.E. Graedel, *Atmospheric corrosion*, John Wiley & Sons, 2000, p. 187.
8. K. Barton, *Protection against atmospheric corrosion. Theories and Methods*, John Willey & Sons, 1976, p. 194.
9. I.L. Rosenfeld and V.P. Persiantseva, Inhibitors of atmospheric corrosion, Moscow: Nauka, 1985, 277 pp. (in Russian)
10. P.D. Donovan, Protection of Metals from Corrosion in Storage and Transit, Chichester, Ellis Horwood Limited, 1986, 228 pp.
11. L.I. Antropov, E.M. Makushin and V.F. Panasenko, *Inhibitors of metal corrosion*, Kiev, Tehnika Publishing House, 1981, 183 pp. (in Russian).
12. J.I. Bregman, *Corrosion inhibitors*, 1963, Pergamon Press, New York.
13. Yu.I. Kuznetsov, *Organic Inhibitors of Corrosion of Metals*, 1996, New York, Plenum Press, 283 pp.
14. O.I. Golyanitsky, *Volatile corrosion inhibitors for ferrous metals*, 1958, Chelyabinsk, Chelyabinsk book publishing house, 75 pp. (in Russian).
15. C. Fiaud, *Theory and practice of vapor phase inhibitors*, in Working Party Report on Corrosion Inhibitors, The Institute of Materials, London, 1994, pp. 1–11.
16. A. Subramanian, M. Natesan, V.S. Muralidharan, K. Balakrishnan and N. Vasudevan, An Overview: Vapor Phase Corrosion Inhibitors, *Corrosion*, 2000, **56**, no. 2, 144–155. doi: 10.5006/1.3280530
17. Yu.I. Kuznetsov, *Fundamental and Practice of Volatile Corrosion Inhibitors of Atmospheric Corrosion of Metals*, in: Proceedings of 6th All Polish Corrosion Conference KORROZJA'99, 1999, p. 425.
18. Yu.I. Kuznetsov and N.N. Andreev, Development of methods for inhibiting the corrosion of metals and new options for their application: a review. Part I. Atmospheric corrosion, *Int. J. Corros. Scale Inhib*., 2023, **12**, no. 4, 2171–2197. doi: 10.17675/2305-6894-2023-12-4-39
19. D.M. Bastidas, E. Cano and E.M. Mora, Volatile Corrosion Inhibitors: a review, *Anti-Corros. Methods Mater*., 2005, **52**, no. 2, 71–77. doi: 10.1108/00035590510584771
20. A.I. Altsybeeva, V.V. Burlov, N.S. Fedorova, T.M. Kuzinova and G.F. Palatik, Volatile inhibitors of atmospheric corrosion of ferrous and nonferrous metals. I. Physical and chemical aspects of selection of starting reagents and synthetic routes, *Int. J. Corros. Scale Inhib*., 2012, **1**, no. 1, 51–64. doi: 10.17675/2305-6894-2012-1-1-051-064
21. A.I. Altsybeeva, V.V. Burlov, N.S. Fedorova, T.M. Kuzinova and G.F. Palatik, Volatile inhibitors of atmospheric corrosion of ferrous and nonferrous metals. II. Prediction of the efficiency of volatile inhibitors of atmospheric corrosion of steel (with Schiff and Mannich bases as examples), *Int. J. Corros. Scale Inhib*., 2012, **1**, no. 2, 99–106. doi: 10.17675/2305-6894-2012-1-2-099-106

22. F.A. Ansari, C. Verma, Y.S. Siddiqui, E.E. Ebenso and M.A. Quraishi, Volatile corrosion inhibitors for ferrous and non-ferrous metals and alloys: A review, *Int. J. Corros. Scale Inhib*., 2018, **7**, no. 2, 126–150. doi: 10.17675/2305-6894-2018-7-2-2
23. S. Gangopadhyay and P.A. Vahanwar, Recent developments in the volatile corrosion inhibitor (VCI) coatings for metal: a review, *J. Coat. Technol. Res*., 2018, **15**, no 4, 789–807. doi: 10.1007/s11998-017-0015-6
24. Yu.I. Kuznetsov, *The Role of Irreversible Adsorption in the Protection Action of Volatile Corrosion Inhibitors*, CORROSION 98, USA, NACE, Houston, San Diego, 1998, Paper No. 242.
25. B. Valdez, M. Schorr, N. Cheng, E. Beltran and R. Beltran, Technological Applications of Volatile Corrosion Inhibitors, *Corros. Rev*., 2018, **36**, no. 3, 227–238. doi: 10.1515/corrrev-2017-0102
26. N.N. Andreev, O.A. Goncharova, Yu.I. Kuznetsov and A.Yu. Luchkin, *A method for metal protection from atmospheric corrosion*, RU Patent 2649354, 02.04.2018 (in Russian).
27. O.A. Goncharova, A.Yu. Luchkin, Yu.I. Kuznetsov, N.N. Andreev, N.P. Andreeva and S.S. Vesely, Octadecylamine, 1,2,3-benzotriazole and a mixture thereof as chamber inhibitors of steel corrosion, *Int. J. Corros. Scale Inhib*., 2018, **7**, no. 2, 203–212. doi: 10.17675/2305-6894-2018-7-2-7
28. O.A. Goncharova, A.Yu. Luchkin, N.P. Andreeva, V.E. Kasatkin, S.S. Vesely, N.N. Andreev and Yu.I. Kuznetsov, Mutual Effects of Components of Protective Films Applied on Steel in Octadecylamine and 1,2,3-Benzotriazole Vapors, *Materials*, 2021, **14**, no. 23, 7181. doi: 10.3390/ma14237181
29. O.A. Goncharova, Yu.I. Kuznetsov, N.N. Andreev, A.Yu. Luchkin, N.P. Andreeva and D.S. Kuznetsov, A new corrosion inhibitor for zinc chamber treatment, *Int. J. Corros. Scale Inhib*., 2018, **7**, no. 3, 340–351. doi: 10.17675/2305-6894-2018-7-3-5
30. O.A. Goncharova, A.Yu. Luchkin, N.N. Andreev, N.P. Andreeva and S.S. Vesely, Triazole derivatives as chamber inhibitors of copper corrosion, *Int. J. Corros. Scale Inhib*., 2018, **7**, no. 4, 657–672. doi: 10.17675/2305-6894-2018-7-4-12
31. F. Mansfeld, M.W. Kending and S. Tsai, Recording and Analysis of AC Impedance Data for Corrosion Studies, *Corrosion*, 1982, **37**, 301–307. doi: 10.5006/1.3577304
32. F. Mansfeld, Use of electrochemical impedance spectroscopy for the study of corrosion protection by polymer coatings, *J. Appl. Electrochem*., 1995, **25**, 187–202. doi: 10.1007/BF00262955
33. *Impedance spectroscopy: theory, experiment, and applications*, Eds.: E. Barsoukov and J.R. Macdonald, 2018, John Wiley & Sons.
34. A.I. Shcherbakov, I.G. Korosteleva, I.V. Kasatkina, V.E. Kasatkin, L.P. Kornienko, V.N. Dorofeeva, V.V. Vysotskii and V.A. Kotenev, Impedance of an Aluminum Electrode with a Nanoporous Oxide, *Prot. Met. Phys. Chem. Surf*., 2019, **55**, 689–694. doi: 10.1134/S2070205119040208

♦ ♦ ♦